https://doi.org/10.20965/jdr.2019.p0744

Paper:

Installation of New GNSS Network Around Kusatsu-Shirane Volcano, Japan: Its Perspective and the First Result

Rina Noguchi[*,**,†], **Tatsuji Nishizawa**[**], **Wataru Kanda**[**], **Takahiro Ohkura**[***], **and Akihiko Terada**[**]

[*]Institute of Space and Astronautical Science, Japan Aerospace Exploration Agency
3-1-1 Yoshinodai, Chuo-ku, Sagamihara, Kanagawa 252-5210, Japan
[†]Corresponding author, E-mail: r-noguchi@planeta.sci.isas.jaxa.jp
[**]Volcanic Fluid Research Center, School of Science, Tokyo Institute of Technology, Tokyo, Japan
[***]Aso Volcanological Laboratory, Graduate School of Science, Kyoto University, Kumamoto, Japan

[Received November 30, 2018; accepted May 12, 2019]

Crustal deformation is essential information for monitoring volcanic activity. In the summit area of the Kusatsu-Shirane Volcano (KSV), a dense Global Navigation Satellite System (GNSS) network has been operating near the recent volcanic center, Yugama crater. This network is sensitive to shallow depth activity, such as phreatic eruptions at the summit area, but is not applicable to deep magmatic activity, suggested to have been occurring for thousands of years by recent geological studies. Aiming to detect magmatic activity at a certain depth, we installed a new GNSS network near KSV. The observation sites were selected based on the crustal deformation pattern calculated for several intrusive events of the deep-seated magma. First, the GNSS sites for campaign observation were installed at eight locations in 2017. Then, four continuous sites commenced operation after a phreatic eruption at Mt. Motoshirane in January 2018. Here, we show the results of the first and second observation campaigns, operating in October 2017 and February 2018. Coordinate values are computed by precise point positioning with ambiguity resolution (PPP-AR) analysis and are used to calculate the displacement and the baseline length change during this period. The uncertainties of the calculated coordinate values are sufficiently small (less than 4.5 mm) except at some sites for which the data possibly include multipath errors due to trees and snow. Although any deformation associated with the 2018 eruption of Mt. Motoshirane is not detected, subsequent observations would contribute to monitoring long-term activity near KSV.

Keywords: Kusatsu-Shirane volcano, global navigation satellite system, crustal deformation, magma reservoir

1. Introduction

The Kusatsu-Shirane volcano (KSV) is one of the active volcanoes in Japan and is known to have a well-developed hydrothermal system which is closely related to phreatic eruptions and seismic activity (e.g., [1–3]). KSV consists of two major peaks: Mt. Shirane and Mt. Motoshirane (**Fig. 1**). Mt. Shirane has three major crater lakes (Yugama, Mizugama, and Karegama). Mt. Motoshirane is composed of four main pyroclastic cones: Ko-Motoshirane, Shin-Motoshirane, Kagami-ike, and Kagami-ike-kita ([4] and references therein). They are all volcanic vents, some of which have fumarolic activity. Between Mt. Shirane and Mt. Motoshirane, there exist several vents, including Ainomine pyroclastic cone and Yumi-ike maar. Yumi-ike maar is thought to have been formed simultaneously with pyroclastic cones in the Mt. Motoshirane area [5]. Recent eruption activity of KSV is represented by phreatic eruptions near Yugama crater at Mt. Shirane. Since the oldest historic eruption of 1882, nineteen phreatic eruptions have been recorded [6]. After the last magmatic eruption at Kagami-ike-kita cone nearly 1500 years ago, the volcanic activity in KSV shifted to the phreatic eruption activity near Yugama crater at Mt. Shirane (e.g., [4]). In other words, KSV is characterized by the more recent phreatic eruptions, which have exhibited continuous magmatic activity at Mt. Motoshirane since approximately 1500 years ago (e.g., [4, 7]). Recent geological studies have revealed magmatic eruptions that caused large amounts of lava effusion during the past thousands of years in KSV [4, 8, 9]. In this background, it is necessary to prepare an observation network to detect the crustal deformation in a wide range leading to a magmatic eruption in the future. For this purpose, we installed a new GNSS network around KSV.

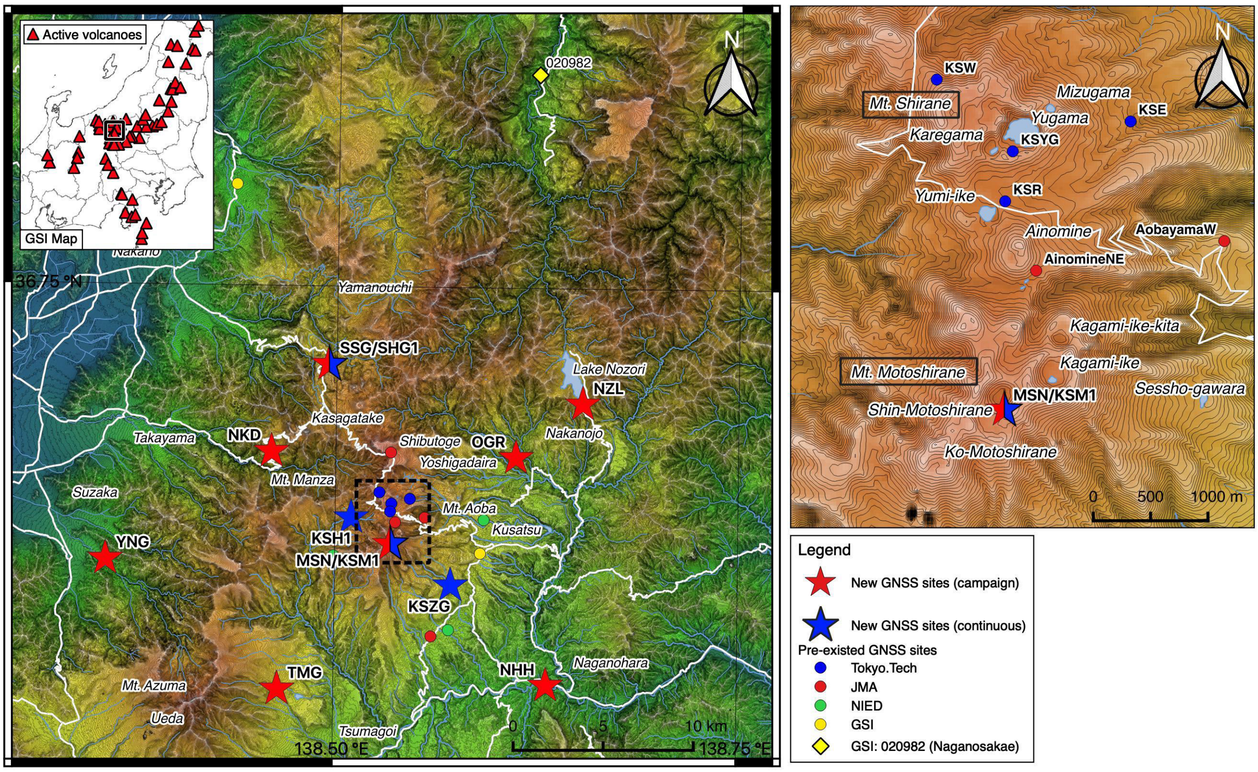

Fig. 1. Newly installed and pre-existing GNSS network around Kusatsu-Shirane Volcano. Black dashed line box in the left side map indicates the region of the right side map. Base map: ALOS Global Digital Surface Model which is 30-m-mesh data, issued by JAXA.

2. Background: Pre-Existing Observation Sites

Since around 2009, the Kusatsu-Shirane Volcano Observatory (KSVO) of the Tokyo Institute of Technology has been studying crustal deformation related to the volcanic activity of KSV, using several observation instruments consisting of seismometers, tiltmeters, and a Global Navigation Satellite System (GNSS) network. Because the recent eruptive activity is characterized by phreatic eruptions in and around Yugama crater [5], the pre-existing observation network was constructed with the aim of detecting shallow crustal deformation near Yugama crater: KSR, KSW, KSE, and KSYG (added in 2011) (**Fig. 1**). Using this GNSS network, crustal deformation associated with volcanic unrest has been observed continuously. The collected data are sent to the data server in KSVO and automatically computed as the daily coordinate values by Spider software (Leica). Whereas this high-density network is sensitive to shallow activity, detection of deep crustal deformation caused by intrusions of magma can be limited. To detect deeper crustal activity, a wider-range observation network is necessary. Furthermore, this concentrated network is vulnerable to eruptions in the summit area. Actually, in the 2018 eruption of Mt. Motoshirane, the observation network faced a crisis of power failure as the commercial power system was destroyed by volcanic explosions. To avoid such a situation, it is meaningful to expand the observation network to locations away from the volcanic center. Besides KSVO, the Geospatial Information Authority of Japan (GSI), Japan Meteorological Agency (JMA), and National Research Institute for Earth Science and Disaster Resilience (NIED) also have continuous GNSS observation sites near KSV (**Fig. 1**). Although data from these other institutions, covering a wide range around KSV, can be used, the observation sites are sparsely distributed. In particular, there are few observation sites within 5–10 km from Yugama crater (**Fig. 1**), which are considered to be essential to detect the crustal deformation caused by the magma activity of KSV. Therefore, we have to increase the spatial density of the GNSS network.

3. Method

3.1. Selection of Observation Sites

To select the location of an observation site to be newly installed, we calculated the uplift height and horizontal displacement associated with a deep magmatic intrusion (modeled as a spherical inflation source) in advance of using the Mogi model [10]. Considering the topography of the volcanic edifice, we used the elevation-corrected Mogi model [11];

$$U_z = \frac{3a^3\Delta P}{4\mu}\frac{D+h}{\{(D+h)^2+r^2\}^{\frac{3}{2}}} \quad \ldots\ldots \quad (1)$$

$$U_r = \frac{3a^3\Delta P}{4\mu}\frac{r}{\{(D+h)^2+r^2\}^{\frac{3}{2}}} \quad . \ . \ . \ . \ . \ . \ . \quad (2)$$

where U_z and U_r are the vertical and horizontal displacements, respectively, a is the radius of the inflation source, D is the depth of inflation source below sea level, h is the height above sea level, ΔP is the pressure change, and μ is the shear modulus. We assumed 1000 m, 1.01325×10^8 Pa, and 40 GPa for a, ΔP, and μ, respectively. These assumptions correspond to a volume increase of 7.85×10^6 m^3. The horizontal and vertical displacements were calculated using MaGCAP-V ver. 1.7 (Magnetic and Geodetic Computer Analysis Processes for Volcano [12]) with varying depths for the inflation source in the range of 0–10 km [11]. **Fig. 2** and **Figs. 4–6** (in **Appendix A**) show examples of calculation results assuming the depth of the inflation source to be 2.5 km, 5.0 km, 7.0 km, and 10.0 km below sea level just beneath Shin-Motoshirane crater or Yugama crater. These results indicate that the crustal deformation associated with deep magmatic intrusions cannot be detected at the pre-existing GNSS observation sites that are concentrated around Yugama crater; thus, it is necessary to disperse the observation sites within 15 km of the summit area. Considering the simulation results and accessibility, we determined the location of ten sites consisting of four continuous sites (KSH1, KSM1, KSZG, and SHG1) and six campaign sites (NHH, TMG, YNG, OGR, NZL, and NKD). **Table ??** shows the locations of those sites and the detailed observation settings. As described later, KSM1 and SHG1 started continuous observation after conversion from campaign observation sites (MSN and SSG, respectively).

3.2. Installation

We installed GNSS observation sites from the summer of 2017 to the autumn of 2018. In 2017, eight sites (MSN, SSG, NHH, TMG, YNG, OGR, NZL, and NKD) were set up for campaign observation. In 2018, four continuous observation sites (including two conversions from the campaign sites) were installed. Six of the campaign observation sites were built using a stainless-steel plate, upon which a tribrach adapter was mounted (**Fig. 7** in **Appendix A**). This stainless-steel plate was attached to a pre-existing building using a rubber sheet so as to track five or more GNSS satellites. For MSN, located at the southern rim of Shin-Motoshirane crater, we fixed a stainless-steel bolt, 6 cm in length, onto a stiff rock constituting a lava dome (**Fig. 7B** in **Appendix A**). For TMG, we buried a pin on the asphalt as a marker for tripod installation (**Fig. 7C** in **Appendix A**). We carried out campaign observations during a calm and dry autumn season without typhoons to avoid a warm and wet climate. During the campaign observation, four sets of GNSS equipment were used to perform a three-day observation twice. Each set of GNSS equipment consists of an antenna (JAVAD GrAnt G3T) and a receiver (JAVAD Sigma G2T). The sampling rate and elevation mask were set at 30 s and 10°, respectively.

In conjunction with the installation of campaign observation sites, we set up the continuous sites around KSV one after another: Shizukayama (KSZG) in March 2018 and Manza (KSH1) in May 2018 (**Fig. 1**). The former is located at approximately 2.5 km WNW from the Yugama crater, and the latter is approximately 5.5 km SE from the crater. In addition, we converted a campaign site (SSG) into the continuous one (SHG1) in May 2018. At these three sites, we installed the GR10 GNSS receiver and AR10 antenna (Leica Geosystems). AR10 is a multipurpose antenna with an integrated radome, which could prevent ash from adhering to the antenna. Finally, we started operating the campaign site (MSN) as a continuous site (KSM1) using the same GNSS equipment used for campaign observation (JAVAD Sigma G2T and GrAnt G3T) in October 2018. The data measured at these continuous observation sites are telemetered using the mobile phone network (Docomo 3G FOMA). Specifically, the Wi-Fi router is turned on by a mechanical timer for only one hour (9:00–10:00 JST) every day to establish an internet connection for the GNSS receiver. During that time, the raw carrier phase and pseudo-range data stored in the receiver are downloaded via FTP from the data server in KSVO. This extension of the GNSS observation network is expected to lead to the detection of a wider range of crustal deformation, caused by inflation of the deep magma reservoir of KSV.

3.3. Data Processing

For data measured by the campaign observation, we performed precise point positioning with ambiguity resolution (PPP-AR) [13] analysis to determine the position of each site; then, we calculated their displacements and the baselines between them. PPP-AR is a positioning technique that is able to compute an accurate solution with a single receiver without any reference stations [13]. Because the raw data were recorded as a JPS file (native format file of JAVAD GNSS receiver), they were converted to a RINEX file using JPS2RIN software (ver. 2.0.112, JAVAD GNSS). Then, the converted RINEX data were used to calculate daily positions in reference to the IGS08 by PPP-AR analysis using GIPSY OASIS II ver. 6.1.2, developed at the NASA Jet Propulsion Laboratory (JPL) [13]. Taking into account the ocean tide loading values, FES2004 was adopted as ocean tide model for each observation site [14]. During the data processing, we also considered the GNSS antenna phase characteristics consisting of antenna phase center offset and phase center variation factor of the antenna. The wet atmospheric delay effect was corrected using the global mapping function (GMF) [15], based on numerical weather model data obtained by JPL. The clock data files were downloaded from the FTP server of the Crustal Dynamics Data Information System (CDDIS), provided by NASA. Calculation of relative displacements and mapping of their spatial distribution were also performed using MaGCAP-V. We adopted the GEONET 020982 site, one of the nationwide GNSS network sites operated by GSI, as the reference site

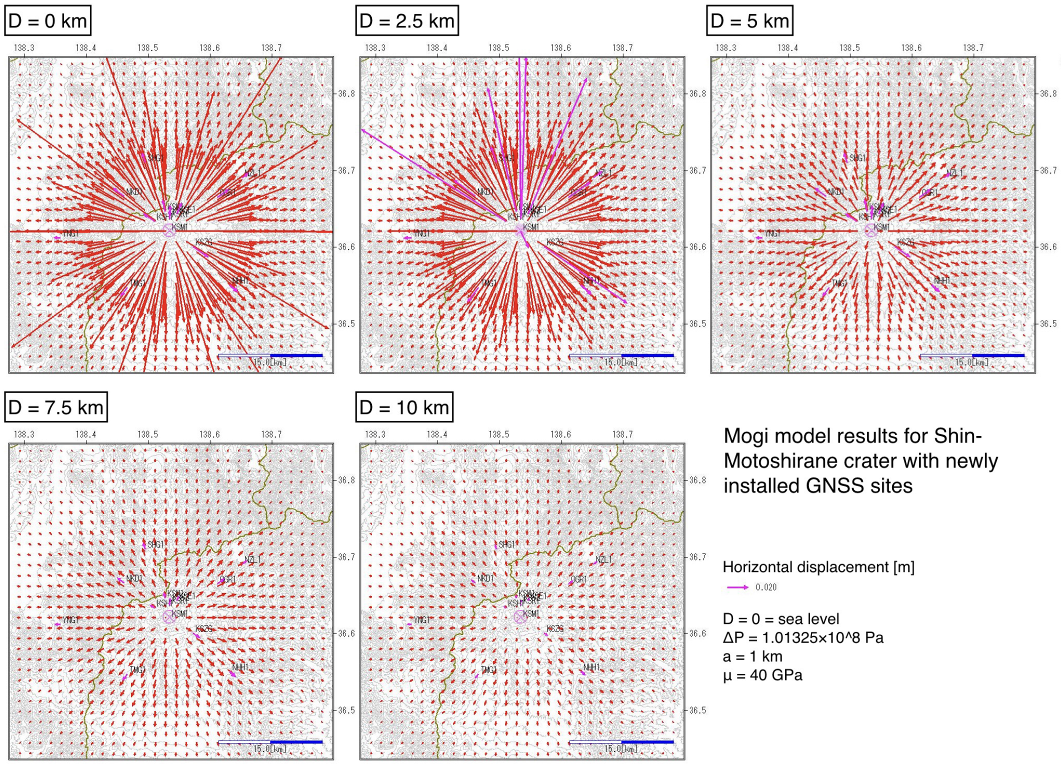

Fig. 2. Distribution of horizontal displacement (red arrow) based on the Mogi model when an inflation source is assumed to be located beneath the Shin-Motoshirane crater at 0, 2.5, 5.0, 7.5, and 10 km below sea level.

Table 1. Description of GNSS stations around Kusatsu-Shirane volcano including pre-existing sites of KSVO.

Site	Place name	in Japanese	Latitude [degree]	Longitude [degree]	Elevation [m]	Continuous/Repeated	Power source
KSZG	Shizukayama	静可山	36.6010	138.5721	1270	Continuous	AC power
KSH1	Manza	万座	36.6344	138.5100	1681	Continuous	AC power
NHH	Naganohara	長野原	36.5514	138.6317	624	Repeated	Battery
TMG	Tsumagoi	嬬恋	36.5481	138.4654	1394	Repeated	Battery
YNG	Yonago	米子	36.6123	138.3577	690	Repeated	Battery
NKD	Kasadake	ニュー笠岳	36.6670	138.4603	1492	Repeated	Battery
SSG/SHG1	Shiga Kogen	志賀高原	36.7108	138.4951	1595	Repeated → Continuous	Solar+Battery
NZL	Nozoriko	野反湖	36.6914	138.6520	1591	Repeated	Battery
OGR	Ogura	小倉	36.6656	138.6115	1150	Repeated	Battery
MSN/KSM1	Motoshirane	本白根	36.6212	138.5347	2135	Repeated → Continuous	Solar+Battery
KSE[1]	Yugama higashi	湯釜東	36.6438	138.5446	1941	Continuous	AC power
KSYG	Yugama	湯釜	36.6413	138.5347	2057	Continuous	AC power
KSR	Rest house	レストハウス	36.6378	138.5344	2012	Continuous	AC power
KSW	Yugama nishi	湯釜西	36.6471	138.5267	2096	Continuous	AC power

[1] Stopped during October 2018 and November 2018.

to calculate the relative displacement so as to remove the common crustal deformation caused mainly by the post-seismic deformation of the 2011 Tohoku-Oki earthquake (e.g., [16]).

To calculate the baseline lengths at each site, we used calculation services provided by GSI (https://vldb.gsi.go.jp/sokuchi/surveycalc/main.html) for two steps of conversion of the coordinate values 1) from earth-centered, earth-fixed (ECEF) to latitude-longitude-geoid height, and 2) from latitude-longitude-geoid height to north-east-up (NEU). For the NEU reference frame, we applied the Japan Plane Rectangular CS (VIII for SHG, NKD, YNG, and IX for NHH, OGR, NZL, TMG, KSM, KSYG, KSR, and KSW). Baseline lengths were calculated using the Pythagorean theorem in three-dimensions.

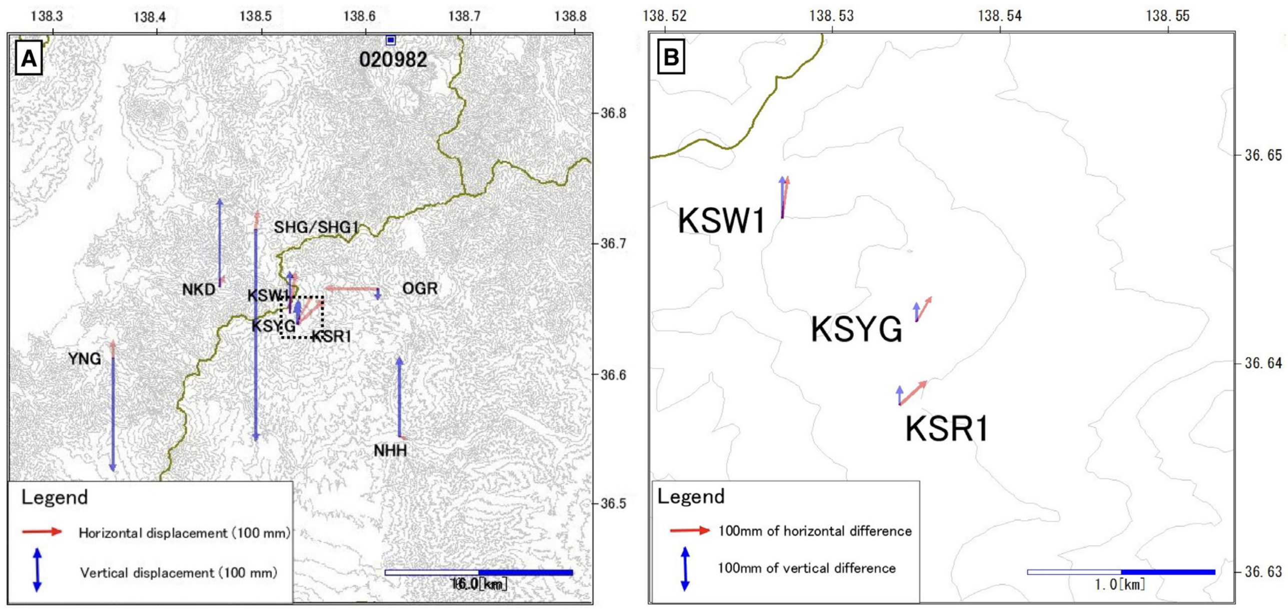

Fig. 3. Displacements during 2017 October to 2018 February around Kusatsu-Shirane Volcano. Dashed rectangle in (A) indicates the region of (B).

4. Results: The First and Second Campaign Observations

The first campaign observation was performed from middle to late October 2017. After the occurrence of a phreatic eruption at Mt. Motoshirane on January 23, 2018 [3], we performed an urgent temporary observation during early February. On account of snow coverage, some sites were inaccessible; eventually, we were able to access only five sites: NHH, YNG, OGR, NKD, and SSG in the latter observation. As described above, we carried out the measurements for more than three days at each site; thus, we analyzed the daily data. Therefore, the mean coordinate values were adopted as the positioning results for the observation period, in which apparent outliers were excluded. **Table 4** (in **Appendix A**) shows the coordinate values of each GNSS observation site, including pre-existing sites of KSVO.

The standard deviations, representing the accuracy of the first campaign observation, are sufficiently small (less than 5.3 mm and 21.7 mm for horizontal and vertical directions, respectively). Given the surrounding circumstances, a multipath error caused by nearby trees is possibly contained in the data at OGR. For the second campaign observation, it is considered that the OGR and SSG data contain multipath errors caused by the surrounding snow.

Figure 3 and **Table 2** show the displacement of each site and the change in baseline length (distance between each site with Naganosakae) between the first campaign observation and the second one. During October 2017 to February 2018, the horizontal displacement shows an eastward trend at all sites, except YNG and OGR. The vertical displacements are positive (i.e., upward) for NHH, NKD, KSYG, KSW, and KSR, and negative (i.e., downward) for OGR, SSG, and YNG. **Table 3** shows changes in the length of each baseline (between each pair, XYZ in reference to the GRS80) during October 2017 to February 2018. The baseline change in this period is less than 18.2 mm. Because our data is not continuous (i.e., campaign observation for a few days) and the scale of the 2018 eruption at Mt. Motoshirane was small, it is nearly impossible to discuss the contribution of the eruptive activity to our data.

Table 2. The amount of displacement relative to the electronic reference point of GSI (Naganosakae, 020982) during October 2017 to February 2018 detected by our GNSS network.

Site	Eastward displacement [mm]	Northward displacement [mm]	Upward displacement [mm]	Baseline change between Naganosakae [mm]
NHH	2.3	−0.9	21.5	0.8
OGR	−14.3	0	−3.1	0.7
SSG	0.7	5.3	−56.6	−6.6
NKD	1.3	3.1	24	−2.8
YNG	−0.1	5	−30.5	−3.5
KSYG	4.1	7	5.4	−7.7
KSW	1.7	11.3	11.5	−10.7
KSR	7.3	6.7	5.4	−8.4

Table 3. Change in baseline length between each site during October 2017 to February 2018 detected by newly built GNSS network.

	Baseline length change [mm]							
	NHH	NKD	OGR	SSG	YNG	KSYG	KSR	KSW
NHH	–	−1.3	4.7	1.0	−6.0	5.8	1.9	11.4
NKD	−1.3	–	10.6	−2.1	8.1	−2.5	−10.8	−4.8
OGR	4.7	10.6	–	13.5	6.7	−10.4	−18.2	−12.8
SSG	1.0	−2.1	13.5	–	4.2	0.6	−7.7	−1.9
YNG	−6.0	8.1	6.7	4.2	–	−5.9	−14.0	−7.6
KSYG	5.8	−2.5	−10.4	0.6	−5.9	–	−2.7	4.0
KSR	1.9	−10.8	−18.2	−7.7	−14.0	−2.7	–	8.9
KSW	11.4	−4.8	−12.8	−1.9	−7.6	4.0	8.9	–

5. Summary and Perspective

We installed GNSS observation sites near Kusatsu-Shirane Volcano in an effort to detect the crustal deformation associated with deep magma intrusion. The first observation result shows that our extended GNSS network works well despite some exceptions due to surrounding circumstances. In the present study, crustal deformation associated with the phreatic eruption at Mt. Motoshirane was not detected. The primary factor is its smallness in eruption scale; however, we also have problems that need improving in terms of analysis. To extract the crustal deformation caused by the magmatic activity of KSV, several influences, such as the 2011 earthquake off the Pacific coast of Tohoku have to be corrected from the measured positioning data. We believe that the continuation of observations would contribute to the monitoring of long-term volcanic activity near Kusatsu-Shirane Volcano.

Acknowledgements

We thank Teruyuki Kato, Yosuke Aoki, Akito Araya, and Masataka Masuda of the Earthquake Research Institute (ERI), the University of Tokyo, for their kind cooperation with the use of GNSS equipment. Masataka Harada helped us to choose observation sites. Yusaku Ohta provided us valuable advice for data analysis. A special thanks to all the landowners of the GNSS sites who allowed us to set up facilities and carry out observations. Drawings for the displacements were performed using MaGCAP-V software, developed at the Meteorological Research Institute of JMA. Critical and constructive comments from the two anonymous referees were highly helpful in improving the original manuscript. This study was supported by the MEXT Integrated Program for Next Generation Volcano Research and Human Resource Development (Y. Morita) and by ERI JULP 2017-G-17 (R. Noguchi).

References:

[1] H. Tsuya, “Explosive activity of volcano Kusatu-Sirane in October, 1932,” Bull. Earthq. Res. Inst., Vol.11, No.1, pp. 82-112,1933.

[2] T. Minakami, K. Matsuita, and S. Utibori, “Explosive activities of volcano Kusatu-Sirane during 1938 and 1942 (Part II),” Bull. Earthq. Res. Inst., Vol.20, No.4, pp. 505-526, 1943.

[3] A. Terada, “Kusatsu-Shirane volcano as a site of phreatic eruptions,” J. Geol. Soc. Japan, Vol.124, No.4, pp. 251-270, 2018 (in Japanese with English abstract).

[4] A. Nigorikawa, Y. Ishizaki, N. Kametani, M. Yoshimoto, A. Terada, K. Ueki, and K. Nakamura, “Holocene eruption history of the Moto-shirane pyroclastic cone group, Kusatsu-Shirane Volcano,” Japan Geosci. Union Meet. 2016 Abst., SVC 48-11, 2016.

[5] Y. Hayakawa and M. Yui, “Eruptive History of the Kusatsu Shirane Volcano,” Quaternary Res., Vol.28, Issue 1, pp. 1-17, 1989 (in Japanese with English abstract).

[6] Japan Meteorological Agency, “44. Kusatsu-Shiranesan,” National Catalogue of the Active Volcanoes in Japan, 4th edition, 25pp., 2013.

[7] M. Yoshimoto, K. Nakamura, A. Nigorikawa, A. Terada, and Y. Ishizaki, “Preliminary report for tephra stratigraphy at the flank of Kusatsu-Shirane volcano,” 2013 Fall Meet. Volcanol. Soc. Japan, Abst., p. 39, 2013 (in Japanese).

[8] N. Kametani, Y. Ishizaki, M. Yoshimoto, and A. Terada, “Holocene eruption history of Kusatsu-Shirane volcano,” Vol. Soc. Japan, 2017, Abst., P084, p. 204, 2017.

[9] N. Kametani, Y. Ishizaki, M. Yoshimoto, and A. Terada, “Eruption history of the Shirane Pyroclastic Cone Group (SPCG), Kusatsu-Shirane volcano, from trench survey and ^{14}C dating: eruption ages of a crater chain and the Yumi-ike maar on the southern foot of the SPCG,” Japan Geosci. Union Meet. 2018 Abst., SVC41-P11, 2018.

[10] K. Mogi, “Relations between eruptions of various volcanoes and the deformations of the ground surfaces around them,” Bull. Earthq. Res. Inst. Vol.36, No.2, pp. 99-134, 1958.

[11] Meteorological Research Institute, “Studies on evaluation method of volcanic activity,” Tech. Rep. Meteorol. Res. Inst., doi:10.11483/mritechrepo.53, 2008 (in Japanese).

[12] K. Fukui, S. Ando, F. Fujiwara, S. Kitagawa, K. Kokubo, S. Onizawa, T. Sakai, T. Shimbori, A. Takagi, T. Yamamoto, H. Yamasato, and A. Yamazaki, “MaGCAP-V: a Windows-based software to analyze ground deformation and geomagnetic change in volcanic areas,” Abstr. IAVCEI, 4W_2C-P8, 2013.

[13] J. F. Zumberge, M. B. Heflin, D. C. Jefferson, M. M. Watkins, and F. H. Webb, “Precise point positioning for the efficient and robust analysis of GPS data from large networks,” J. Geophys. Res., Solid Earth, Vol.102, No.B3, pp. 5005-5017, 1997.

[14] F. Lyard, F. Lefevre, T. Letellier, and O. Francis, “Modelling the global ocean tides: modern insights from FES2004,” Ocean Dynam., Vol.56, No.5-6, pp. 394-415, 2006.

[15] J. Boehm, A. Niell, P. Tregoning, and H. Schuh, “Global Mapping Function (GMF): a new empirical mapping function based on numerical weather model data,” Geophys. Res. Lett. Vol.33, No.7, L07304, 2006.

[16] A. Hashima, T. W. Becker, A. M. Freed, H. Sato, and D. A. Okaya, “Coseismic deformation due to the 2011 Tohoku-oki earthquake: influence of 3-D elastic structure around Japan,” Earth, Planets and Space, Vol.68, No.1, Article: 159, 2016.

Appendix A. Supplementary Figures and Table

Figures 4–6 present the calculation results based on Mogi model and **Fig. 7** shows observation sites. **Table 4** shows the coordinate values of each GNSS observation site.

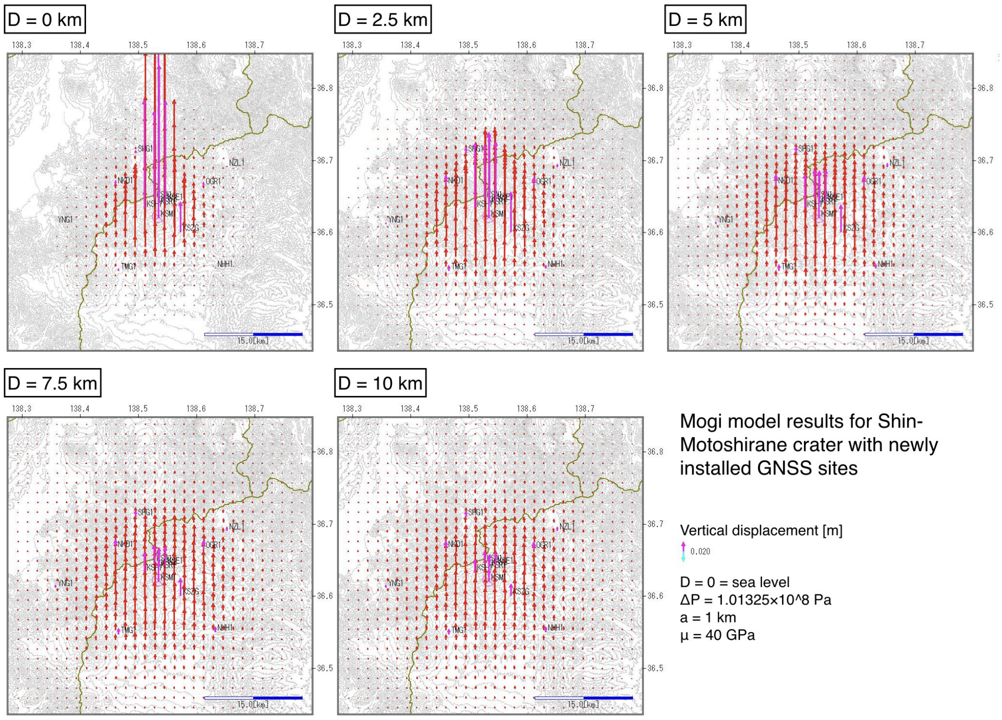

Fig. 4. Distribution of vertical displacement (red arrow) based on the Mogi model when an inflation source is assumed to be located beneath the Shin-Motoshirane crater at 0, 2.5, 5.0, 7.5, and 10 km below sea level.

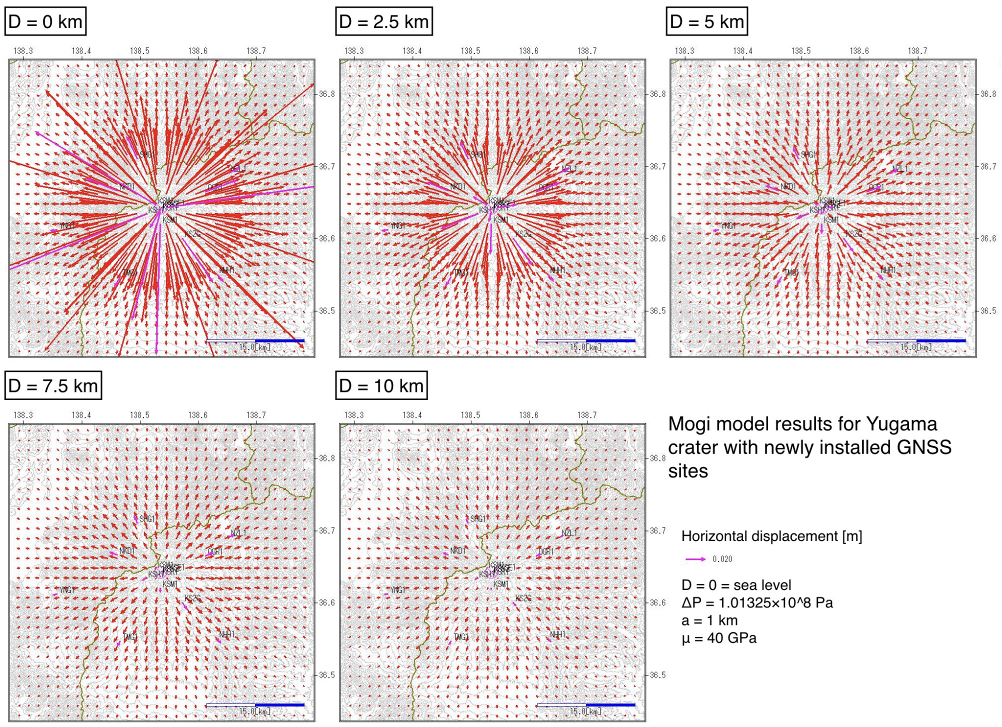

Fig. 5. Distribution of horizontal displacement (red arrow) based on the Mogi model when an inflation source is assumed to be located beneath the Yugama crater at 0, 2.5, 5.0, 7.5, and 10 km below sea level.

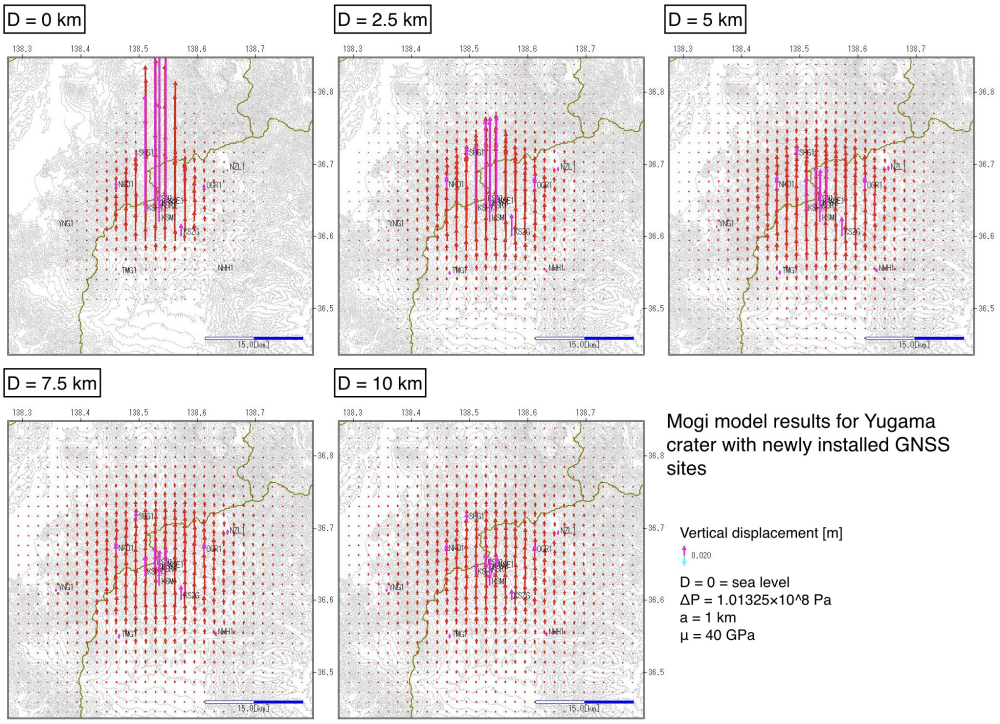

Fig. 6. Distribution of vertical displacement (red arrow) based on the Mogi model when an inflation source is assumed to be located beneath the Yugama crater at 0, 2.5, 5.0, 7.5, and 10 km below sea level.

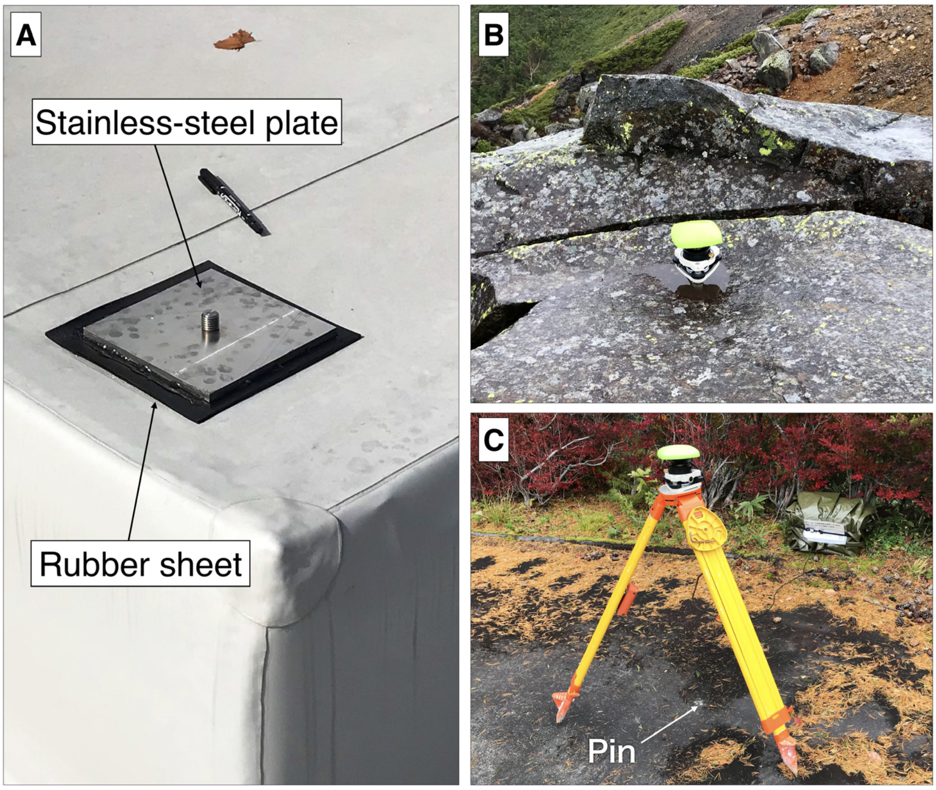

Fig. 7. Photos of observation sites. A: NHH, B: MSN, and C: TMG.

Table 4. Coordinate values by newly built GNSS campaign network.

Site	Japan Plane Rectangular	ECEF WGS-84										GRS80			NEU GRS-80 (IX)				NEU GRS-80 (VIII)				Coordinate values. NEU GRS-80 (VIII/IX) (north-east-up)					
		ID	Year	Month	Day	X [m]	Y [m]	Z [m]		No.	Use or not	Latitude (DMS)	Longitude (DMS)	Ellipsoid height [m]	X [m]	Y [m]	True north bearing (dms)	Scale factor	X [m]	Y [m]	True north bearing (dms)	Scale factor	X [m]	Y [m]	Z [m]	sdX [m]	sdY [m]	sdZ [m]
NHH	IX	NHH1	2017	10	16	-3850201.6069	3390629.0424	3777920.3706	17	NHH-1	○	363304.98138	1383754.00612	677.973	61849.5968	-107578.8655	4256.56	1.00004254	61185.7577	11787.3391	-442.29	0.99990171	61849.5968	-107578.8673	677.9806	0.0007	0.0016	0.0076
		NHH1	2017	10	17	-3850201.6086	3390629.0444	3777920.3734	17	NHH-2	○	363304.98140	1383754.00610	677.976	61849.5975	-107578.8660	4256.56	1.00004254	61185.7583	11787.3386	-442.29	0.99990171						
		NHH1	2017	10	18	-3850201.6127	3390629.0493	3777920.3781	17	NHH-3	○	363304.98140	1383754.00606	677.984	61849.5975	-107578.8670	4256.56	1.00004254	61185.7583	11787.3376	-442.29	0.99990171						
		NHH1	2017	10	19	-3850201.6067	3390629.0479	3777920.3717	17	NHH-4	○	363304.98134	1383754.00594	677.976	61849.5957	-107578.8700	4256.56	1.00004254	61185.7564	11787.3347	-442.29	0.99990171						
		NHH1	2017	10	20	-3850201.6185	3390629.0562	3777920.3834	17	NHH-5	○	363304.98137	1383754.00601	677.994	61849.5966	-107578.8682	4256.56	1.00004254	61185.7574	11787.3364	-442.29	0.99990171						
		NHH1	2018	2	3	-3850201.6049	3390629.0321	3777920.3629	18	NHH-6	○	363304.98134	1383754.00637	677.961	61849.5955	-107578.8593	4256.56	1.00004254	61185.7565	11787.3453	-442.29	0.99990171	61849.5951	-107578.8570	677.9727	0.0008	0.0031	0.0119
		NHH1	2018	2	4	-3850201.6091	3390629.0356	3777920.3674	18	NHH-7	○	363304.98135	1383754.00638	677.968	61849.5958	-107578.8590	4256.56	1.00004254	61185.7568	11787.3456	-442.29	0.99990171						
		NHH1	2018	2	5	-3850201.6269	3390629.0425	3777920.3782	18	NHH-8	○	363304.98129	1383754.00664	677.989	61849.5939	-107578.8526	4256.56	1.00004254	61185.7549	11787.3521	-442.29	0.99990171						
OGR	IX	OGR1	2017	10	16	-3843649.6493	3387261.9946	3788400.1817	17	OGR-1	○	363956.00050	1383641.40439	1194.412	74541.6148	-109223.2657	4346.85	1.00004693	73851.9169	9967.2141	-359.7	0.99990122	74541.6141	-109223.2676	1194.4213	0.0007	0.0018	0.0155
		OGR1	2017	10	17	-3843649.6451	3387261.9920	3788400.1766	17	OGR-2	○	363956.00046	1383641.40436	1194.405	74541.6135	-109223.2665	4346.85	1.00004693	73851.9157	9967.2133	-359.7	0.99990122						
		OGR1	2017	10	18	-3843649.6690	3387262.0143	3788400.2024	17	OGR-3	○	363956.00050	1383641.40432	1194.446	74541.6148	-109223.2675	4346.85	1.00004693	73851.9169	9967.2123	-359.7	0.99990122						
		OGR1	2017	10	19	-3843649.6533	3387262.0044	3788400.1871	17	OGR-4	○	363956.00045	1383641.40420	1194.422	74541.6133	-109223.2705	4346.85	1.00004693	73851.9153	9967.2094	-359.7	0.99990122						
		OGR1	2017	10	20	-3843650.5054	3387263.9680	3788401.4967	17	OGR-5	×	363955.99700	1383641.36757	1196.759	74541.5185	-109224.1814	4346.87	1.00004693	73851.8080	9966.2999	-359.67	0.99990122						
		OGR1	2018	2	3	-3843649.6148	3387261.9699	3788400.1558	18	OGR-6	○	363956.00064	1383641.40422	1194.362	74541.6191	-109223.2699	4346.85	1.00004693	73851.9212	9967.2099	-359.7	0.99990122	74541.6168	-109223.2705	1194.3780	0.0023	0.0005	0.0160
		OGR1	2018	2	4	-3843649.6352	3387261.9892	3788400.1709	18	OGR-7	○	363956.00049	1383641.40418	1194.394	74541.6145	-109223.2710	4346.85	1.00004693	73851.9166	9967.2089	-359.7	0.99990122						
		OGR1	2018	2	5	-3916960.1183	3390074.7774	3827176.5187	18	OGR-8	×	363820.57908	1390727.35435	70126.247	71139.1724	-63406.5598	2523.4	0.99994952	71086.5128	55823.1693	-2221.19	0.99993838						
NZL	IX	NZL1	2017	10	16	-3845020.8165	3383649.6612	3790962.5219	17	NZL-1	○	364128.96696	1383907.05444	1635.563	77361.9361	-105571.1224	4221.39	1.00003727	76722.3317	13579.2919	-526.87	0.99990227	77361.9333	-105571.1211	1635.5612	0.0033	0.0027	0.0080
		NZL1	2017	10	17	-3845020.8231	3383649.6629	3790962.5165	17	NZL-2	○	364128.96671	1383907.05457	1635.564	77361.9284	-105571.1193	4221.39	1.00003727	76722.3240	13579.2952	-526.87	0.99990227						
		NZL1	2017	10	18	-3845020.8209	3383649.6656	3790962.5259	17	NZL-3	○	364128.96695	1383907.05443	1635.57	77361.9358	-105571.1227	4221.39	1.00003727	76722.3313	13579.2917	-526.87	0.99990227						
		NZL1	2017	10	19	-3845020.8157	3383649.6632	3790962.5221	17	NZL-4	○	364128.96696	1383907.05436	1635.563	77361.9361	-105571.1244	4221.39	1.00003727	76722.3317	13579.2899	-526.87	0.99990227						
		NZL1	2017	10	20	-3845020.8130	3383649.6506	3790962.5072	17	NZL-5	○	364128.96677	1383907.05467	1635.546	77361.9302	-105571.1168	4221.39	1.00003727	76722.3258	13579.2977	-526.87	0.99990227						
TMG	IX	TMG1	2017	10	24	-3840963.9061	3402336.8419	3778083.1721	17	TMG-1	○	363253.25697	1382755.38683	1438.952	61687.0463	-122471.2556	4852.96	1.00008474	60816.8829	-3098.9452	114.21	0.99990012	61687.0450	-122471.2556	1438.9593	0.0013	0.0018	0.0054
		TMG1	2017	10	25	-3840963.9106	3402336.8491	3778083.1770	17	TMG-2	○	363253.25694	1382755.38674	1438.961	61687.0455	-122471.2579	4852.96	1.00008474	60816.8819	-3098.9474	114.21	0.99990012						
		TMG1	2017	10	26	-3840963.9170	3402336.8487	3778083.1778	17	TMG-3	○	363253.25687	1382755.38692	1438.965	61687.0432	-122471.2534	4852.96	1.00008474	60816.8798	-3098.9429	114.21	0.99990012						
SHG	VIII	SHG1	2017	10	24	-3834787.0996	3393314.7709	3792696.8066	17	SHG-1	○	364238.84063	1382942.44939	1647.145	79699.9518	-119556.9698	4800.16	1.00007605	78865.2634	-435.5414	10.49	0.9999	78865.2617	-435.5426	1647.1468	0.0017	0.0013	0.0018
		SHG1	2017	10	25	-3834787.1013	3393314.7761	3792696.8045	17	SHG-2	○	364238.84049	1382942.44928	1647.148	79699.9475	-119556.9725	4800.16	1.00007605	78865.2591	-435.5441	10.49	0.9999						
		SHG1	2017	10	26	-3834787.1005	3393314.7715	3792696.8045	17	SHG-3	○	364238.84056	1382942.44940	1647.145	79699.9496	-119556.9695	4800.16	1.00007605	78865.2613	-435.5412	10.49	0.9999						
		SHG1	2017	10	27	-3834787.1006	3393314.7747	3792696.8083	17	SHG-4	○	364238.84062	1382942.44930	1647.149	79699.9515	-119556.9720	4800.16	1.00007605	78865.2631	-435.5436	10.49	0.9999						
		SHG1	2018	2	5	-3834787.0636	3393314.7319	3792696.7808	18	SHG-5	○	364238.84099	1382942.44961	1647.087	79699.9628	-119556.9641	4800.16	1.00007605	78865.2745	-435.5360	10.49	0.9999	78865.2693	-435.5321	1647.0727	0.0050	0.0029	0.0217
		SHG1	2018	2	6	-3834787.0694	3393314.7308	3792696.7790	18	SHG-6	○	364238.84087	1382942.44980	1647.089	79699.9590	-119556.9595	4800.16	1.00007605	78865.2708	-435.5312	10.49	0.9999						
		SHG1	2018	2	7	-3834787.0460	3393314.7070	3792696.7438	18	SHG-7	○	364238.84060	1382942.44989	1647.042	79699.9507	-119556.9574	4800.16	1.00007605	78865.2625	-435.5290	10.49	0.9999						
NKD	VIII	NKD1	2017	10	24	-3834830.0573	3397513.6310	3788739.0218	17	NKD-1	○	364001.34918	1382736.99846	1540.321	74889.3250	-122739.9726	4912.15	1.00008555	74011.7192	-3550.7816	125.4	0.99990016	74011.7158	-3550.7829	1540.3230	0.0045	0.0019	0.0065
		NKD1	2017	10	25	-3834830.0526	3397513.6297	3788739.0178	17	NKD-2	○	364001.34916	1382736.99838	1540.315	74889.3245	-122739.9746	4912.15	1.00008555	74011.7186	-3550.7836	125.4	0.99990016						
		NKD1	2017	10	26	-3834830.0600	3397513.6322	3788739.0213	17	NKD-3	○	364001.34911	1382736.99850	1540.323	74889.3229	-122739.9717	4912.15	1.00008555	74011.7171	-3550.7807	125.4	0.99990016						
		NKD1	2017	10	27	-3834830.0670	3397513.6450	3788739.0203	17	NKD-4	○	364001.34882	1382736.99830	1540.333	74889.3140	-122739.9768	4912.15	1.00008555	74011.7081	-3550.7856	125.4	0.99990016						
		NKD1	2018	2	3	-3834830.0619	3397513.6277	3788739.0352	18	NKD-5	○	364001.34950	1382736.99868	1540.33	74889.3348	-122739.9670	4912.15	1.00008555	74011.7291	-3550.7762	125.4	0.99990016	74011.7261	-3550.7753	1540.3224	0.0025	0.0016	0.0114
		NKD1	2018	2	4	-3834830.0639	3397513.6265	3788739.0342	18	NKD-6	○	364001.34947	1382736.99877	1540.33	74889.3339	-122739.9648	4912.15	1.00008555	74011.7282	-3550.7739	125.4	0.99990016						
		NKD1	2018	2	5	-3834830.0627	3397513.6271	3788739.0321	18	NKD-7	○	364001.34942	1382736.99872	1540.328	74889.3323	-122739.9661	4912.15	1.00008555	74011.7266	-3550.7752	125.4	0.99990016						
		NKD1	2018	2	6	-3834830.0631	3397513.6254	3788739.0266	18	NKD-8	○	364001.34929	1382736.99879	1540.324	74889.3283	-122739.9644	4912.15	1.00008555	74011.7226	-3550.7734	125.4	0.99990016						
		NKD1	2018	2	7	-3834830.0457	3397513.6154	3788739.0134	18	NKD-9	○	364001.34933	1382736.99862	1540.3	74889.3296	-122739.9686	4912.15	1.00008555	74011.7238	-3550.7777	125.4	0.99990016						
YNG	VIII	YNG1	2017	10	24	-3830962.8346	3406351.3229	3783383.7924	17	YNG-1	○	363644.40212	1382127.65102	730.962	68954.5923	-132005.1594	5248.73	1.00011462	67950.0786	-12730.8185	505.56	0.999902	67950.0784	-12730.8188	730.9540	0.0013	0.0017	0.0057
		YNG1	2017	10	25	-3830962.8241	3406351.3169	3783383.7851	17	YNG-2	○	363644.40216	1382127.65092	730.949	68954.5935	-132005.1618	5248.73	1.00011462	67950.0799	-12730.8210	505.56	0.999902						
		YNG1	2017	10	26	-3830962.8299	3406351.3165	3783383.7841	17	YNG-3	○	363644.40206	1382127.65109	730.951	68954.5904	-132005.1577	5248.73	1.00011462	67950.0768	-12730.8168	505.56	0.999902						
		YNG1	2017	10	27	-3830962.7380	3406351.4045	3783383.8118	17	YNG-4	×	363644.40298	1382127.64599	730.96	68954.6207	-132005.2840	5248.73	1.00011462	67950.1053	-12730.9434	505.57	0.999902						
		YNG1	2018	2	5	-3830962.8183	3406351.3100	3783383.7809	18	YNG-5	○	363644.40223	1382127.65098	730.939	68954.5957	-132005.1603	5248.73	1.00011462	67950.0820	-12730.8195	505.56	0.999902	67950.0829	-12730.8148	730.9273	0.0020	0.0035	0.0172
		YNG1	2018	2	6	-3830962.8232	3406351.3066	3783383.7810	18	YNG-6	○	363644.40220	1382127.65121	730.94	68954.5947	-132005.1546	5248.73	1.00011462	67950.0811	-12730.8138	505.56	0.999902						
		YNG1	2018	2	7	-3830962.8006	3406351.2828	3783383.7623	18	YNG-7	○	363644.40235	1382127.65132	730.903	68954.5993	-132005.1518	5248.73	1.00011462	67950.0857	-12730.8110	505.56	0.999902						
KSM1	IX	KSM1	2017	10	16	-3841906.5172	3394888.2661	3785038.5654	17	KSM-1	○	363716.14757	1383204.85035	2188.161	69704.4463	-116157.4863	4629.14	1.00006618	68919.6686	3101.9203	-114.48	0.99990012	69704.4457	-116157.4869	2188.1628	0.0017	0.0028	0.0079
		KSM1	2017	10	17	-3841906.5177	3394888.2605	3785038.5584	17	KSM-2	○	363716.14745	1383204.85053	2188.155	69704.4425	-116157.4819	4629.14	1.00006618	68919.6649	3101.9248	-114.48	0.99990012						
		KSM1	2017	10	18	-3841906.5148	3394888.2656	3785038.5642	17	KSM-3	○	363716.14758	1383204.85030	2188.159	69704.4466	-116157.4875	4629.14	1.00006618	68919.6689	3101.9191	-114.48	0.99990012						
		KSM1	2017	10	19	-3841906.5247	3394888.2780	3785038.5747	17	KSM-4	○	363716.14755	1383204.85019	2188.178	69704.4457	-116157.4903	4629.14	1.00006618	68919.6680	3101.9163	-114.48	0.99990012						
		KSM1	2017	10	20	-3841906.5152	3394888.2670	3785038.5660	17	KSM-5	○	363716.14760	1383204.85027	2188.161	69704.4472	-116157.4883	4629.14	1.00006618	68919.6696	3101.9183	-114.48	0.99990012						
KSYG	IX	KSYG	2017	10	16	-3840854.2080	3393952.2214	3786784.6376	##	KSYG-1	○	363828.84058	1383205.03657	2099.770	71945.1040	-116122.5522	4630.35	1.00006608					71945.1067	-116122.5542	2099.7542	0.0018	0.0017	0.0172
		KSYG	2017	10	17	-3840854.1877	3393952.2040	3786784.6194	##	KSYG-2	○	363828.84062	1383205.03655	2099.737	71945.1052	-116122.5526	4630.35	1.00006608										
		KSYG	2017	10	18	-3840854.1829	3393952.2015	3786784.6193	##	KSYG-3	○	363828.84072	1383205.03650	2099.733	71945.1083	-116122.5538	4630.35	1.00006608										
		KSYG	2017	10	19	-3840854.1951	3393952.2144	3786784.6324	##	KSYG-4	○	363828.84072	1383205.03643	2099.755	71945.1083	-116122.5556	4630.35	1.00006608										
		KSYG	2017	10	20	-3840854.2073	3393952.2267	3786784.6447	##	KSYG-5	○	363828.84070	1383205.03639	2099.776	71945.1077	-116122.5566	4630.35	1.00006608										
		KSYG	2018	2	3	-3840854.1902	3393952.1943	3786784.6293	##	KSYG-6	○	363828.84097	1383205.03691	2099.740	71945.1159	-116122.5436	4630.35	1.00006608					71945.1137	-116122.5440	2099.7374	0.0015	0.0009	0.0050
		KSYG	2018	2	4	-3840854.1851	3393952.1896	3786784.6227	##	KSYG-7	○	363828.84093	1383205.03692	2099.730	71945.1146	-116122.5433	4630.35	1.00006608										
		KSYG	2018	2	5	-3840854.1881	3393952.1955	3786784.6259	##	KSYG-8	○	363828.84089	1383205.03682	2099.737	71945.1134	-116122.5458	4630.35	1.00006608										
		KSYG	2018	2	6	-3840854.1952	3393952.1985	3786784.6288	##	KSYG-9	○	363828.84083	1383205.03692	2099.745	71945.1116	-116122.5434	4630.35	1.00006608										
		KSYG	2018	2	7	-3840854.1883	3393952.1932	3786784.6240	##	KSYG-10	○	363828.84087	1383205.03689	2099.735	71945.1128	-116122.5441	4630.35	1.00006608										
KSR1	IX	KSR1	2017	10	16	-3840983.8023	3394106.5516	3786447.8577	##	KSR1-1	○	363816.21950	1383203.83595	2058.709	71556.4694	-116157.6405	4630.84	1.00006618					71556.4718	-116157.6436	2058.7072	0.0021	0.0037	0.0147
		KSR1	2017	10	17	-3840983.7923	3394106.5399	3786447.8480	##	KSR1-2	○	363816.21955	1383203.83604	2058.691	71556.4709	-116157.6382	4630.84	1.00006618										
		KSR1	2017	10	18	-3840983.7871	3394106.5440	3786447.8497	##	KSR1-3	○	363816.21961	1383203.83578	2058.691	71556.4729	-116157.6447	4630.84	1.00006618										
		KSR1	2017	10	19	-3840983.8018	3394106.5593	3786447.8623	##	KSR1-4	○	363816.21953	1383203.83571	2058.716	71556.4704	-116157.6465	4630.84	1.00006618										
		KSR1	2017	10	20	-3840983.8063	3394106.5652	3786447.8739	##	KSR1-5	○	363816.21969	1383203.83565	2058.729	71556.4754	-116157.6479	4630.84	1.00006618										
		KSR1	2018	2	3	-3840983.7998	3394106.5287	3786447.8606	##	KSR1-6	○	363816.21991	1383203.83658	2058.698	71556.4818	-116157.6247	4630.84	1.00006618					71556.4803	-116157.6252	2058.6948	0.0011	0.0013	0.0044
		KSR1	2018	2	4	-3840983.7951	3394106.5255	3786447.8555	##	KSR1-7	○	363816.21989	1383203.83655	2058.690	71556.4812	-116157.6254	4630.84	1.00006618										
		KSR1	2018	2	5	-3840983.7984	3394106.5314	3786447.8593	##	KSR1-8	○	363816.21986	1383203.83646	2058.697	71556.4803	-116157.6277	4630.84	1.00006618										
		KSR1	2018	2	6	-3840983.8031	3394106.5307	3786447.8596	##	KSR1-9	○	363816.21981	1383203.83661	2058.700	71556.4788	-116157.6240	4630.84	1.00006618										
		KSR1	2018	2	7	-3840983.7961	3394106.5248	3786447.8534	##	KSR1-10	○	363816.21983	1383203.83660	2058.689	71556.4794	-116157.6242	4630.84	1.00006618										
KSW1	IX	KSW1	2017	10	16	-3840115.5424	3394258.8239	3787325.2069	##	KSW1-1	○	363849.68972	1383136.10522	2141.218	72597.5215	-116832.4721	4648.00	1.00006812					72597.5213	-116832.4765	2141.2168	0.0011	0.0053	0.0077
		KSW1	2017	10	17	-3840115.5425	3394258.8198	3787325.2034	##	KSW1-2	○	363849.68968	1383136.10534	2141.213	72597.5202	-116832.4692	4648.00	1.00006812										
		KSW1	2017	10	18	-3840115.5334	3394258.8218	3787325.2025	##	KSW1-3	○	363849.68977	1383136.10504	2141.209	72597.5231	-116832.4766	4648.00	1.00006812										
		KSW1	2017	10	19	-3840115.5342	3394258.8290	3787325.2029	##	KSW1-4	○	363849.68967	1383136.10484	2141.213	72597.5201	-116832.4816	4648.00	1.00006812										
		KSW1	2017	10	20	-3840115.5435	3394258.8393	3787325.2151	##	KSW1-5	○	363849.68972	1383136.10478	2141.231	72597.5216	-116832.4831	4648.00	1.00006812										
		KSW1	2018	2	3	-3840115.5411	3394258.8122	3787325.2196	##	KSW1-6	○	363849.69022	1383136.10554	2141.218	72597.5368	-116832.4640	4648.00	1.00006812					72597.5358	-116832.4642	2141.2136	0.0008	0.0011	0.0045
		KSW1	2018	2	4	-3840115.5380	3394258.8082	3787325.2144	##	KSW1-7	○	363849.69019	1383136.10557	2141.211	72597.5359	-116832.4633	4648.00	1.00006812										
		KSW1	2018	2	5	-3840115.5335	3394258.8084	3787325.2126	##	KSW1-8	○	363849.69020	1383136.10545	2141.207	72597.5362	-116832.4662	4648.00	1.00006812										
		KSW1	2018	2	6	-3840115.5435	3394258.8131	3787325.2184	##	KSW1-9	○	363849.69015	1383136.10557	2141.219	72597.5346	-116832.4633	4648.00	1.00006812										
		KSW1	2018	2	7	-3840115.5385	3394258.8097	3787325.2150	##	KSW1-1(	○	363849.69017	1383136.10554	2141.213	72597.5353	-116832.4640	4648.00	1.00006812										

Name:
Rina Noguchi

Affiliation:
Researcher, Institute of Space and Astronautical Science, Japan Aerospace Exploration Agency

Address:
3-1-1 Yoshinodai, Chuo-ku, Sagamihara, Kanagawa 252-5210, Japan

Brief Career:
2015- Institute of Space and Astronautical Science, Japan Aerospace Exploration Agency
2015- Geological Survey of Japan, National Institute of Advanced Industrial Science and Technology
2016- Volcanic Fluid Research Center, School of Science, Tokyo Institute of Technology
2018- Institute of Space and Astronautical Science, Japan Aerospace Exploration Agency

Selected Publications:
• R. Noguchi and K. Kurita, "Unique characteristics of cones in Central Elysium Planitia, Mars," Planetary and Space Science, Vol.111, pp. 44-54, 2015.
• R. Noguchi, A. Höskuldsson, and K. Kurita, "Detailed topographical, distributional, and material analyses of rootless cones in Myvatn, Iceland,"J. of Volcanology and Geothermal Research, Vol.318, pp. 89-102, 2016.
• D. Shoji, R. Noguchi, S. Otsuki, and H. Hino, "Classification of volcanic ash particles using a convolutional neural network and probability," Nature, Scientific Reports, Vol.8, Article No.8111, 2018.

Academic Societies & Scientific Organizations:
• Volcanological Society of Japan (VSJ)
• Japan Geoscience Union (JpGU)

Name:
Tatsuji Nishizawa

Affiliation:
Researcher, Volcanic Fluid Research Center, School of Science, Tokyo Institute of Technology

Address:
2-12-1 Ookayama, Meguro-ku, Tokyo 152-8551, Japan

Brief Career:
2018- Volcanic Fluid Research Center, School of Science, Tokyo Institute of Technology

Selected Publications:
• T. Nishizawa, H. Nakamura, T. Churikova, B. Gordeychik, O. Ishizuka, S. Haraguchi, T. Miyazaki, B. S. Vaglarov, Q. Chang, M. Hamada, J.-I. Kimura, K. Ueki, C. Toyama, A. Nakao, and H. Iwamori, "Genesis of ultra-high-Ni olivine in high-Mg andesite lava triggered by seamount subduction," Nature, Scientific Reports, Vol.7, Article No.11515, doi:10.1038/s41598-017-10276-3, 2017.

Academic Societies & Scientific Organizations:
• Volcanological Society of Japan (VSJ)
• Japan Geoscience Union (JpGU)

Name:
Wataru Kanda

Affiliation:
Associate Professor, Volcanic Fluid Research Center, School of Science, Tokyo Institute of Technology

Address:
641-36, Kusatsu, Agatsuma, Gunma 377-1711, Japan

Brief Career:
1998- Research Associate, Disaster Prevention Research Institute, Kyoto University
2010- Associate Professor, Volcanic Fluid Research Center, Tokyo Institute of Technology
2016- Associate Professor, School of Science, Tokyo Institute of Technology

Selected Publications:
• W. Kanda et al., "A Heating Process of Kuchi-erabu-jima Volcano, Japan, as Inferred from Geomagnetic Field Variations and Electrical Structure," J. Volcanol. Geotherm. Res., Vol.189, No.1-2, pp. 158-171, 2010.
• W. Kanda et al., "Hydrothermal system of the active crater of Aso volcano (Japan) inferred from a three-dimensional resistivity structure model," Earth, Planets and Space, Vol.71, No.1, Article: 37, 2019.

Academic Societies & Scientific Organizations:
• Volcanological Society of Japan (VSJ)
• Japan Geoscience Union (JpGU)
• Society of Geomagnetism and Earth, Planetary and Space Sciences (SGEPSS)
• Society of Economic Geologists (SEG)

Name:
Takahiro Ohkura

Affiliation:
Professor, Aso Volcanological Laboratory, Institute for Geothermal Sciences, Graduate School of Science, Kyoto University

Address:
3028 Sakanashi, Ichinomiyamachi, Aso, Kumamoto 869-2611, Japan

Brief Career:
1991- Kyoto University

Academic Societies & Scientific Organizations:
• Volcanological Society of Japan (VSJ)

Name:
Akihiko Terada

Affiliation:
Lecturer, Volcanic Fluid Research Center, School of Science, Tokyo Institute of Technology

Address:
2-12-1 Ookayama, Meguro-ku, Tokyo 152-8551, Japan

Brief Career:

2003- Institute of Seismology and Volcanology, Faculty of Science, Hokkaido University

2006- Aso Volcanological Laboratory, Graduate School of Science, Kyoto University

2009- Volcanic Fluid Research Center, School of Science, Tokyo Institute of Technology

Selected Publications:

- A. Terada and Y. Ida, "Kinematic features of isolated volcanic clouds revealed by video records," Geophys. Res. Lett., Vol.34, No.1, L01305, doi:10.1029/2006GL026827, 2007.
- A. Terada, T. Hashimoto, and T. Kagiyama, "A water flow model of the active crater lake at Aso volcano, Japan: fluctuations of magmatic gas and groundwater fluxes from the underlying hydrothermal system," Bulletin of Volcanology, Vol.74, No.3, pp. 641-655, 2012.
- A. Terada and T. Hashimoto, "Variety and sustainability of volcanic lakes: Response to subaqueous thermal activity predicted by numerical model," J. Geophys. Res., Solid Earth, Vol.122, No.8, pp. 6108-6130, 2017.

Academic Societies & Scientific Organizations:

- Volcanological Society of Japan (VSJ)
- American Geophysical Union (AGU)
- Geothermal Research Society of Japan (GRSJ)